Chemical Methodologies 4(2020) 40-54

Chemical Methodologies

Journal homepage: http://chemmethod.com

Original Research article

Adsorption of Tetryl on the Surface of $B_{12}N_{12}$: A Comprehensive DFT Study

Mohammad Reza Jalali Sarvestani[a], Roya Ahmadi[b*]

[a] Young Researchers and Elite Club, Yadegar-e-Imam Khomeini(RAH) Shahr-e-Rey Branch, Islamic Azad University, Tehran, Iran
[b] Department of Chemistry, Yadegar-e-Imam Khomeini (RAH) Shahre-rey Branch, Islamic Azad University, Tehran, Iran

ARTICLE INFORMATION

Received: 16 February 2019
Received in revised: 25 March 2019
Accepted: 27 June 2019
Available online: 18 August 2019

DOI: 10.33945/SAMI/CHEMM.2020.1.4

KEYWORDS

Boron nitride cage
Density functional theory
Adsorption
Tetryl
Detection

ABSTRACT

In this study, the adsorption of tetryl on the surface of boron nitride cage was evaluated by density functional theory. For this purpose, the structures of tetryl, $B_{12}N_{12}$, and the tetryl-$B_{12}N_{12}$ complexes were geometrically optimized. Then, IR and frontier molecular orbital calculations were performed on them. The calculated adsorption energies, Gibbs free energy changes (ΔG_{ad}), adsorption enthalpy changes (ΔH_{ad}) and thermodynamic equilibrium constants (K_{th}) revealed that the adsorption process of both explosives is experimentally feasible, spontaneous, exothermic and non-equilibrium. The specific heat capacity values (C_V) showed that the heat sensitivity has been significantly reduced in the tetryl complexes with $B_{12}N_{12}$. The N-O and C-N bond lengths and the density values demonstrated that tetryl-derived products with boron nitride cage have higher explosive velocity and blasting pressure in comparison to the pure blasting materials without $B_{12}N_{12}$. The frontier molecular orbital parameters such as band gap, chemical hardness, electrophilicity, chemical potential and charge capacity were also studied and the results proved that boron nitride cage is an ideal electroactive sensing material in order to fabricate novel sensors for the determination of tetryl.

Corresponding author: E-mail: roya.ahmadi.chem@gmail.com, Department of Chemistry, Yadegar-e-Imam Khomeini (RAH) Shahre-rey Branch, Islamic Azad University, Tehran, Iran, Tel: +98912 2976055; Fax: +9821 33810305

Graphical Abstract

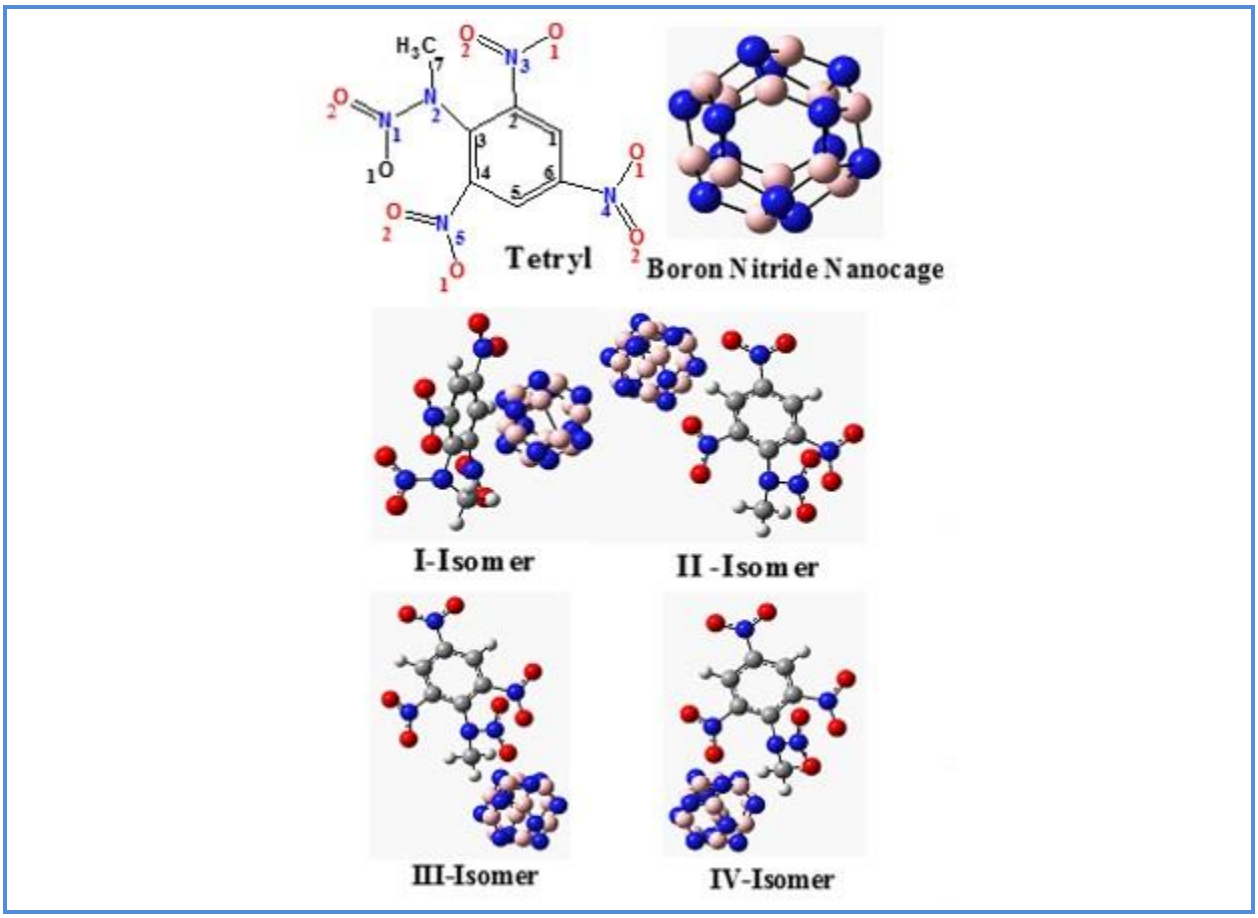

Introduction

Designing new methods for accurate determination and efficient removal of nitro aromatic explosives is of vital importance. The previous studies showed that the settings that are near to ammunition plants, military munition sites and drowned warships are more susceptible to become polluted by nitro aromatic organic compounds which are commonly utilized in the production of war weapons and bombs [1-3]. Nitro aromatic energetic materials are usually released in the environment *via* inadequate disposal techniques, open detonations and explosive combustion. Tetryl whose chemical structure is given in Figure 1, is a highly toxic nitro aromatic explosive. Several studies were carried out on the effects of this compound on the health of humans and other living organisms [4-6]. The results showed that exposure to trace amounts of tetryl can lead to liver damage, nausea, allergenic dermatitis, anemia, blood damage, cataracts, discoloration of skin and hair, tingling sensation in the nose, skin rashes and irritation, severe headaches, nosebleeds, fatigue and weight loss [7-9]. Moreover, most of the nitro aromatic substances are mutagenic and

carcinogenic. The perniciousness of this type of contaminants is attributed to the oxidation stress which can be created by the synthesis of nitro anion radicals and their redox cycling in the body [10-12]. In this regard, the removal and determination of tetryl is very important. The next matter that accentuates the determination of nitro aromatic chemicals is that many terroristic groups which use explosive bombs and detection of the blasting substances can provide a clue for terroristic activities [13].

Various analytical methods such as high-performance liquid chromatography (HPLC), gas chromatography (GC), fluorescence spectroscopy and mass spectrometry (MS) have been developed for the quantitation of nitro aromatic blasting compounds. On the contrary, the disadvantages make their use challengeable because they are based on costly and intricate instrumentation, all of them are time-consuming and require experienced operators. In addition, the referred techniques consume high amounts of toxic organic solvents and suffer from lack of selectivity [14-16]. Fortunately, sensors are ideally portable and small devices that can be referred to as prominent alternatives for the complicated established methods. In recent years, sensors gathered huge attention all over the world, because of their simplicity, high selectivity, acceptable sensitivity, wide linear working range, being economical, applicability in opaque and coloured samples and short analysis time. But, the most important step in the development of a new sensor is to find a chemical recognition element that interacts strongly with the analyte and this interaction should lead to a change in a measurable property in the local environment near the surface of the transducer [17-27]. On the other hand, boron nitride cage (Figure 1 (b)) is a nanostructure with prominent traits such as high thermal stability, low dielectric constant, great thermal conductance, oxidation resistance, specific surface/area ratio and superb structural stability that make it a suitable adsorbent for the removal of various contaminants and an ideal candidate for the detection of various analytes. Accordingly, the adsorption of HCN, OCN^-, amphetamine, proline amino acid and N_2O on the surface of boron nitride cage has been evaluated [28-38].

The next subject that supports investigating the interaction of $B_{12}N_{12}$ with tetryl is that some of the former studies showed nanomaterials which can improve the reactivity and energetic features of explosives and reduce their heat sensitivity in some cases [39-44]. Hence, the goal of this study is to evaluate the adsorption of tetryl on the surface of boron nitride cage by density functional theory as it is for the first time.

Experimental

Computational methods

At first, the structures of tetryl, boron nitride cage and the tetryl-$B_{12}N_{12}$ complexes were designed by Gauss View 3.1 and nanotube modeller 1.3.0.3 Softwares. Afterward, geometrical optimizations, IR and frontier molecular orbital computations were performed on them using the density functional theory method in the B3LYP/6-31G (d) level of theory. This basis set was selected because in former studies, it had produced results which were in an admissible agreement with the experimental data [31-40]. All of the calculations were done in the temperature range of 278.15-378.15 at 10° intervals by Spartan software, in the aqueous phase. The investigated processes were as follows:

$$Tetryl + B_{12}N_{12} \rightarrow Tetryl - B_{12}N_{12} \quad (1)$$

Equations 2-6 were used for calculating adsorption energy values (E_{ad}) and thermodynamic parameters of the evaluated process including enthalpy changes (ΔH_{ad}), Gibbs free energy variations (ΔG_{ad}), thermodynamic constant (K_{th}) and entropy variations (ΔS_{ad}).

$$E_{ad} = \left(E_{(\text{Tetryl}-B_{12}N_{12})} - \left(E_{(\text{Tetryl})} + E_{(B_{12}N_{12})}\right)\right) \quad (2)$$

$$\Delta H_{ad} = \left(H_{(\text{Tetryl}-B_{12}N_{12})} - \left(H_{(\text{Tetryl})} + H_{(B_{12}N_{12})}\right)\right) \quad (3)$$

$$\Delta G_{ad} = \left(G_{(\text{Tetryl}-B_{12}N_{12})} - \left(G_{(\text{Tetryl})} + G_{(B_{12}N_{12})}\right)\right) \quad (4)$$

$$K_{th} = exp(-\Delta G_{ad}/RT) \quad (5)$$

$$\Delta S_{ad} = \left(S_{(\text{Tetryl}-B_{12}N_{12})} - \left(S_{(\text{Tetryl})} + S_{(B_{12}N_{12})}\right)\right) \quad (6)$$

In the aforementioned equations, E represents the total electronic energy of each structure, H denotes the sum of the thermal enthalpy and total energy of the evaluated materials. The G also stands for the sum of the thermal Gibbs free energy and total energy for each of the studied structures. The S represents thermal entropy for each material, R and T are also ideal gas constants and temperature respectively.

Frontier molecular orbital parameters such as band gap (HLG), chemical hardness (η), chemical potential (μ), electrophilicity (ω) and the maximum transferred charge (ΔN_{max}) were calculated via equations 5-9.

$$HLG = E_{LUMO} - E_{HOMO} \quad (7)$$

$$\eta = (E_{LUMO} - E_{HOMO})/2 \quad (8)$$

$$\mu = (E_{LUMO} + E_{HOMO})/2 \quad (9)$$

$$\omega = \mu^2/2_{\mu} \quad (10)$$

$$\Delta N_{max} = -\mu/\eta \quad (11)$$

E_{LUMO} and E_{HOMO} in equations 5 to 7 denote the energy of the lowest unoccupied molecular orbital and the energy of the highest occupied molecular orbital respectively.

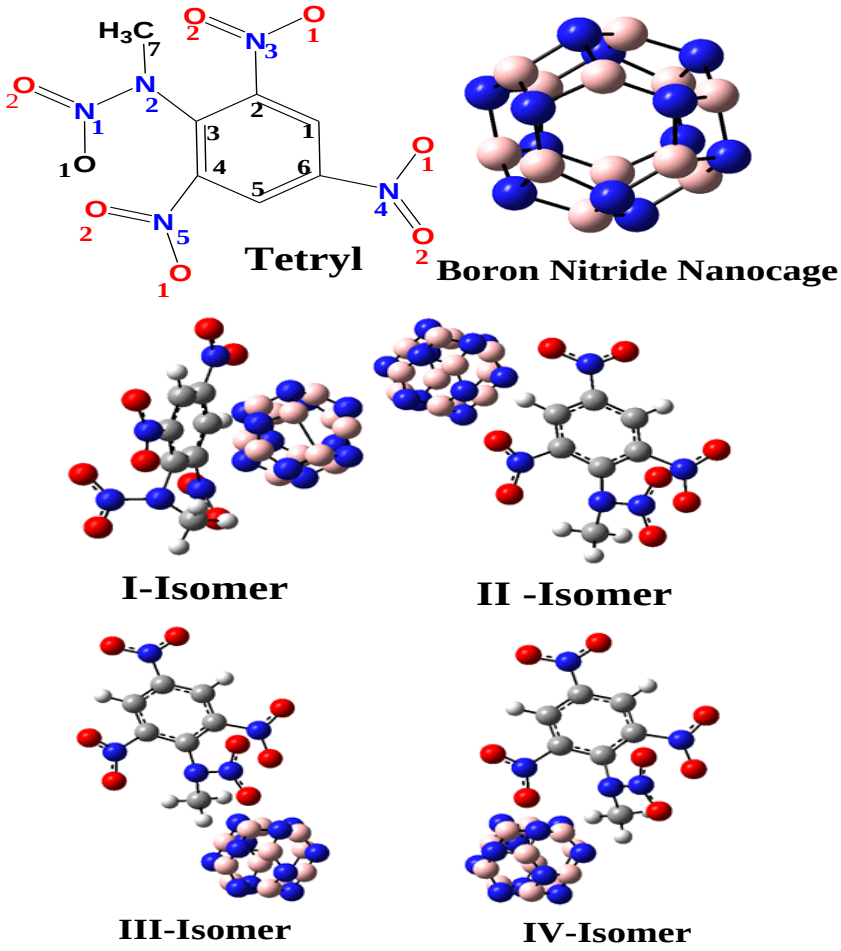

Figure 1. The chemical structure of tetryl and optimized structures of $B_{12}N_{12}$ and its complexes with tetryl at four different configurations

Results and discussion

Structural properties

As can be seen from Figure 1, tetryl was inserted near the boron nitride cage at four different positions, for more convenient understanding, each configuration was remarked by an abbreviated name. The naming method is explained in the following:

The I-Isomer abbreviation was considered for the derivative in which the benzene ring is inserted in parallel form near the $B_{12}N_{12}$ surface. The II-Isomer symbol was also assigned to the derived product that was originated from placing the boron nitride cage near to the first carbon atom of tetryl. The next derivative which was formed by situating the 7th carbon of the methyl group of tetryl near the surface of $B_{12}N_{12}$ was remarked by III-Isomer. IV-Isomer also represents the last configuration in which the third nitrogen atom of tetryl's nitro group is placed near the surface of the boron nitride cage. The reported adsorption energy values in Table 1, were calculated *via* equation 2. As can be seen from the Table, this parameter is considerably negative for all of the configurations, therefore, it can be deduced that the adsorption process of tetryl is experimentally feasible [26-36]. Therefore, this nanostructure can be applied for the removal of this nitroaromatic contaminant from the environmental specimens.

Owing to the fact that N-O, N-NO_2 and C-NO_2 bond lengths are appropriate standards for estimating the blasting power in the nitroaromatic explosives, after implementing geometrical optimization on the studied structures, the mentioned bond lengths were measured and tabulated in Table 1. As the provided data in Table 1 clearly reveal, the N-O, N-NO_2 and C-NO_2 bond lengths have increased in tetryl after being adsorbed on the surface of boron nitride cage at all of the evaluated derivatives. The incrementing of the referred bond lengths exhibits that the existed bonds between nitrogen and oxygen as well as nitrogen and carbon have become much weaker and they can be ruptured more easily by interacting with boron nitride cage. In other words, tetryl derivatives with $B_{12}N_{12}$ can take part in the combustion reaction more conveniently in comparison to the pure explosive and their blasting power have ameliorated substantially [33-35]. Density was the next investigated structural parameter which was obtained by dividing the weight of the structures to the calculated volumes after the optimization step. According to equations 12 and 13, density has a direct and obvious relationship with explosion velocity and detonation pressure [39].

$$D^{1/4} = 1.01\left(NM^{1/2}Q^{1/2}\right)^{1/2}(1 + 1.30\rho) \quad (12)$$

$$P^{1/4} = 1.558NM^{1/2}Q^{1/2}\rho^2 \quad (13)$$

In these formulas, D is the explosion velocity, P is the detonation pressure, M represents the average molecular weight of gaseous products, N stands for the number of moles of gaseous explosion products per gram of explosives, Q is the blasting Heat and ρ is the density of blasting

material. As can be seen from the table, the density of tetryl has enhanced after adsorbing on the surface of $B_{12}N_{12}$. Among the studied derivatives, I-Isomer has the highest density. Hence, coating tetryl on the surface of boron nitride cage leads to a significant rise in the explosion velocity and detonation pressure of the inspected blasting material in all of the configurations [40].

Table 1. The values of the total energy, adsorption energy, lowest frequency, bond lengths, weight, volume and density for tetryl and its complexes with $B_{12}N_{12}$

	Tetryl	I-Isomer	II -Isomer	III-Isomer	IV-Isomer
Total energy (a.u)	-1123.575	-2007.645	-2007.687	-2007.548	-2007.915
Adsorption energy (KJ/mol)	---	-407.215	-517.701	-152.317	-1117.478
Lowest frequency (cm^{-1})	31.169	15.392	27.387	26.581	28.689
C_2-N_3 (Å)	1.512	1.521	1.533	1.522	1.585
C_4-N_5 (Å)	1.507	1.517	1.514	1.517	1.526
C_6-N_4 (Å)	1.515	1.522	1.531	1.523	1.540
N_2-N_1 (Å)	1.477	1.490	1.483	1.484	1.480
N_1-O_1 (Å)	1.276	1.290	1.282	1.291	1.292
N_1-O_2 (Å)	1.268	1.282	1.281	1.282	1.278
N_3-O_1 (Å)	1.512	1.584	1.539	1.551	1.545
N_3-O_2 (Å)	1.236	1.283	1.392	1.243	1.270
N_4-O_1 (Å)	1.275	1.282	1.291	1.286	1.287
N_4-O_2 (Å)	1.279	1.291	1.286	1.294	1.293
N_5-O_1 (Å)	1.278	1.290	1.397	1.291	1.356
N_5-O_2 (Å)	1.277	1.294	1.289	1.285	1.345
C_5-B (Å)	---	1.615	---	---	---
C_5-N (Å)	---	---	1.411	---	---
C_7-B (Å)	---	---	---	1.613	---
C_7-N (Å)	---	---	---	---	1.297
Weight (amu)	287.144	569.945	569.945	569.945	569.945
Volume ($Å^3$)	220.210	426.180	433.300	429.910	431.030
Density=m/v (amu/$Å^3$)	1.304	1.337	1.315	1.326	1.322

Thermodynamic parameters of the adsorption process

The reported ΔH_{ad} values in Table 2, which was calculated from equation 3, clearly indicate that the interaction of boron nitride cage with tetryl is extremely exothermic at all of the configurations. Indeed, the heat or energy is transferred from the system to the environment in the adsorption process of tetryl. In this regard, $B_{12}N_{12}$ can be utilized for the detection of tetryl by thermal sensors. These types of sensors determinate the amount of analyte by measuring the alterations in the environmental temperature by a sensitive thermistor [41, 42]. Among the evaluated derivatives, IV-Isomer has the most negative ΔH_{ad} value which shows that the formation of this configuration is more exothermic and experimentally feasible in comparison to other derived products. The influence of temperature on this parameter was also investigated. As it is obvious from the Table, by increasing of temperature, ΔH_{ad} does not experience any meaningful variations. Therefore, on

the basis of this parameter, the optimum temperature for the adsorption process cannot be determined [31].

The reported ΔG_{ad} values in Table 2 which were calculated from equation 4, exhibit that the interaction of boron nitride cage with tetryl is spontaneously at all of the configurations because of the achieved negative Gibbs free energy alterations. The impact of changing the temperature on this parameter was also checked out and the findings demonstrate that by rising of temperature, ΔG_{ad} has gradually incremented. In other words, the adsorption process has become less spontaneous with temperature increasing. In this regard, 278.15 K was selected as the optimum temperature for the adsorption of tetryl on the surface of boron nitride cage. This phenomenon was not out of expecting because tetryl and is more reactive at higher temperatures and it has more tendency to participate in explosive reactions. However, in lower temperatures, they are more stable and consequently can take part in other interactions more conveniently [32-36].

Table 2. The values of enthalpy changes and Gibbs free energy changes for the adsorption process of tetryl on the surface of $B_{12}N_{12}$ in the temperature range of 278.15-378.15 K

ΔH_{ad} (KJ/mol)				
Temperature (K)	**I-Isomer**	**II-Isomer**	**III-Isomer**	**IV-Isomer**
278.15	-444.128	-559.458	-188.003	-1299.619
288.15	-444.427	-559.682	-188.358	-1299.996
298.15	-444.722	-559.908	-188.686	-1300.342
308.15	-445.009	-560.137	-188.981	-1300.657
318.15	-445.291	-560.363	-189.258	-1300.980
328.15	-445.533	-560.550	-189.521	-1301.278
338.15	-445.755	-560.729	-189.764	-1301.574
348.15	-445.974	-560.898	-189.972	-1301.864
358.15	-446.177	-561.059	-190.172	-1302.131
368.15	-446.376	-561.189	-190.363	-1302.362
378.15	-446.572	-561.306	-190.536	-1302.603
ΔG_{ad} (KJ/mol)				
Temperature (K)	**I-Isomer**	**II-Isomer**	**III-Isomer**	**IV-Isomer**
278.15	-362.512	-480.018	-103.444	-1210.601
288.15	-359.573	-477.220	-100.462	-1207.528
298.15	-356.619	-474.450	-97.522	-1204.479
308.15	-353.726	-471.668	-94.578	-1201.476
318.15	-350.804	-468.825	-91.594	-1198.441
328.15	-347.801	-465.949	-88.556	-1195.340
338.15	-344.856	-463.140	-85.534	-1192.279
348.15	-341.885	-460.265	-82.437	-1189.233
358.15	-338.909	-457.371	-79.384	-1186.221
368.15	-335.922	-454.426	-76.371	-1183.229
378.15	-332.916	-451.448	-73.355	-1180.193

As can be observed from the presented thermodynamic constants in Table 3, tetryl adsorption process is irreversible, one-sided and non-equilibrium. The main advantage of this K_{th} is that it can show the impact of temperature more evidently than other thermodynamic parameters. As it is

obvious, the thermodynamic constant values have reduced significantly by increasing of temperature. The values of adsorption entropy changes (ΔS_{ad}) were also calculated by equation 6 and the results are tabulated in Table 3. As can be seen, this parameter is negative for all of the evaluated configurations which indicate that tetryl interaction with $B_{12}N_{12}$ is inappropriate due to the aggregation in tetryl complexes with boron nitride cage [37-40].

Table 3. The values of thermodynamic constant and entropy changes for the adsorption process of tetryl on the surface of $B_{12}N_{12}$ in the temperature range of 278.15-378.15 K

K_{th}				
Temperature (K)	**I-Isomer**	**I-Isomer**	**I-Isomer**	**I-Isomer**
278.15	$2.818\times10^{+117}$	$2.818\times10^{+117}$	$2.818\times10^{+117}$	$2.818\times10^{+117}$
288.15	$6.896\times10^{+112}$	$6.896\times10^{+112}$	$6.896\times10^{+112}$	$6.896\times10^{+112}$
298.15	$3.423\times10^{+108}$	$3.423\times10^{+108}$	$3.423\times10^{+108}$	$3.423\times10^{+108}$
308.15	$3.310\times10^{+104}$	$3.310\times10^{+104}$	$3.310\times10^{+104}$	$3.310\times10^{+104}$
318.15	$5.664\times10^{+100}$	$5.664\times10^{+100}$	$5.664\times10^{+100}$	$5.664\times10^{+100}$
328.15	$1.596\times10^{+97}$	$1.596\times10^{+97}$	$1.596\times10^{+97}$	$1.596\times10^{+97}$
338.15	$7.448\times10^{+93}$	$7.448\times10^{+93}$	$7.448\times10^{+93}$	$7.448\times10^{+93}$
348.15	$5.354\times10^{+90}$	$5.354\times10^{+90}$	$5.354\times10^{+90}$	$5.354\times10^{+90}$
358.15	$5.756\times10^{+87}$	$5.756\times10^{+87}$	$5.756\times10^{+87}$	$5.756\times10^{+87}$
368.15	$8.939\times10^{+84}$	$8.939\times10^{+84}$	$8.939\times10^{+84}$	$8.939\times10^{+84}$
378.15	$1.943\times10^{+82}$	$1.943\times10^{+82}$	$1.943\times10^{+82}$	$1.943\times10^{+82}$
ΔS_{ad} (J/mol K)				
Temperature (K)	**I-Isomer**	**II-Isomer**	**III-Isomer**	**IV-Isomer**
278.15	-293.584	-285.759	-304.171	-320.207
288.15	-294.634	-286.327	-305.193	-321.072
298.15	-295.645	-286.772	-305.919	-321.688
308.15	-296.375	-287.237	-306.502	-322.018
318.15	-297.129	-287.857	-307.119	-322.451
328.15	-297.963	-288.417	-307.818	-322.981
338.15	-298.518	-288.726	-308.371	-323.359
348.15	-299.106	-289.175	-309.007	-323.652
358.15	-299.632	-289.633	-309.462	-323.769
368.15	-300.149	-290.116	-309.760	-323.731
378.15	-300.678	-290.630	-310.004	-323.838

Due to the fact that the specific heat capacity has an obvious and direct relationship with heat sensitivity, this parameter was also calculated and presented in Table 4. Specific heat capacity is defined as the heat or energy, which is required for raising the temperature of a certain amount of material to one Celsius degree. Therefore, a compound with higher C_V will have a lower sensitivity to the heat because it needs more energy to increase its temperature. On the other hand, a molecule with a low specific heat capacity value will be more sensitive to heat because its temperature can be enhanced by a lower amount of heat. As the provided results in the table obviously reveal, the specific heat capacity has dramatically increased after the adsorption of tetryl on the surface of boron nitride cage, in all of the derivatives [41-45]. Therefore, the heat sensitivity has declined tangibly after tetryl adsorption on the $B_{12}N_{12}$. The next point which can be perceived from the

tables is that by increasing of temperature specific heat capacity values have also augmented linearly.

Table 4. The specific heat capacity values for tetryl and its complexes with $B_{12}N_{12}$ in the temperature range of 278.15-378.15 K

C_V (J/mol.K)					
Temperature (K)	**Tetryl**	**I-Isomer**	**II-Isomer**	**III-Isomer**	**IV-Isomer**
278.15	240.376	420.705	428.910	413.074	399.273
288.15	246.136	434.702	442.947	427.337	413.674
298.15	251.824	448.565	456.825	441.471	427.956
308.15	257.440	462.282	470.534	455.459	442.103
318.15	262.986	475.840	484.065	469.289	456.100
328.15	268.461	489.229	497.409	482.948	469.936
338.15	273.866	502.439	510.559	496.425	483.597
348.15	279.200	515.460	523.507	509.710	497.074
358.15	284.463	528.285	536.247	522.795	510.355
368.15	289.654	540.907	548.773	535.670	523.433
378.15	294.772	553.319	561.082	548.330	536.299

Frontier molecular orbital analysis

As stated before, in chemistry, HOMO is described as the highest occupied molecular orbital and LUMO is defined as the lowest unoccupied molecular orbital, and the energy discrepancy between these orbitals is known as band gap (HLG) which can be calculated *via* equation 7. Determination of this variable is important because of its relevance to the conductivity. Indeed, the compounds with lower values of HLG demand less energy for transmitting their electrons from the ground state to the excited one in comparison to the materials with higher values of the band gap. Hence, a molecule with a little value of HLG will be more conductive than a compound with a high amount of energy gap. As it can be observed from the density of states (DOS) diagrams in Figure 2 and the provided data in Table 5, this parameter has abated significantly after the adsorption of tetryl on the surface of boron nitride cage. In other words, the conductivity has increased remarkably by the interaction of $B_{12}N_{12}$ with tetryl. Therefore, it can be concluded that this nanostructure can be used for the detection of this toxic explosive by conductometric electrochemical sensors [46]. The second investigated parameter was chemical hardness (η) which was calculated by equation 8. This variable has a clear relationship with the reactivity. In fact, the soft molecules that have lower values of η will be more reactive because they can alter their electron density so conveniently, and electronic transmissions that are essential for the implementation of reaction can be done more easily in them. The presented results in the table indicate that the reactivity of tetryl has improved considerably after the adsorbing of tetryl on the $B_{12}N_{12}$. The chemical potential (μ) which is necessary for acquiring other indices was also calculated by equation 9.

Table 5. The calculated E_H and E_L, HLG, chemical hardness (η) , electrophilicity index (ω), and the maximum amount of electronic charge index (ΔN_{max}), dipole moment and zero-point energy for tetryl and its complexes boron nitride cage

	E_H (eV)	E_L (eV)	HLG (eV)	η (eV)	μ (eV)	ω (eV)	ΔN_{max} (eV)	Dipole moment (deby)	Zero-point energy (KJ/mol)
Tetryl	-8.154	2.660	10.814	5.407	-2.747	0.698	0.508	3.170	444.080
Boron nitride cage	-8.290	6.690	14.980	7.490	-0.800	0.043	0.107	0.000	349.518
I-Isomer	-7.194	1.411	8.605	4.303	-2.892	0.972	0.672	3.729	877.067
II-Isomer	-3.515	2.916	6.431	3.215	-0.299	0.014	0.093	14.481	763.855
III-Isomer	-7.594	1.388	8.982	4.491	-3.103	1.072	0.691	3.397	773.550
IV-Isomer	-4.115	2.505	6.621	3.310	-0.805	0.098	0.243	8.595	823.630

Electrophilicity (ω) and maximum transferred charge (ΔN_{max}) that were calculated by equations 10 and 11 consecutively, show the tendency of a molecule towards electron. If a material has a great and positive value of ω and ΔN_{max} it will have more tendency to absorb an electron. However, if a molecule has a low amount of these indices, it will act as an electron donor [47]. The obtained results in the tables reveal that tetryl can act as a Lewis acid or an electron acceptor because of their high electrophilicity and maximum transferred charge values. While, boron nitride cage can play the role of an electron donor due to its low electrophilicity, hence, it can be elicited that the nanostructure and the explosive can take part in electron transfer reactions. Thus, boron nitride cage is an ideal electroactive sensing material for the fabrication of novel tetryl sensitive electrochemical sensors.

Dipole moment is the last investigated parameter. The dipole moment is a key clue which demonstrates the solubility of the investigated structures. A substance with higher dipole moment will have stronger solubility in the polar solvents like water. On the other hand, a low amount of dipole moment indicates the poor solubility in polar solvents. As can be seen, the dipole moment of $B_{12}N_{12}$ is zero, so, this nanostructure is insoluble in water. This fact is of great importance because many sensors lose their sensitivity, stability and selectivity after a short period of time because of the leakage of the recognition element from the membrane to the sample solution. In this regard, sensing materials with lower solubility in polar solvents are more suitable for the construction of new sensors. Fortunately, boron nitride cage meets this requirement. Besides, the dipole moment of

tetryl has enhanced significantly after its interaction with $B_{12}N_{12}$. So, it can be deduced that tetryl has become more soluble in water after the adsorbing on the surface of boron nitride cage [48].

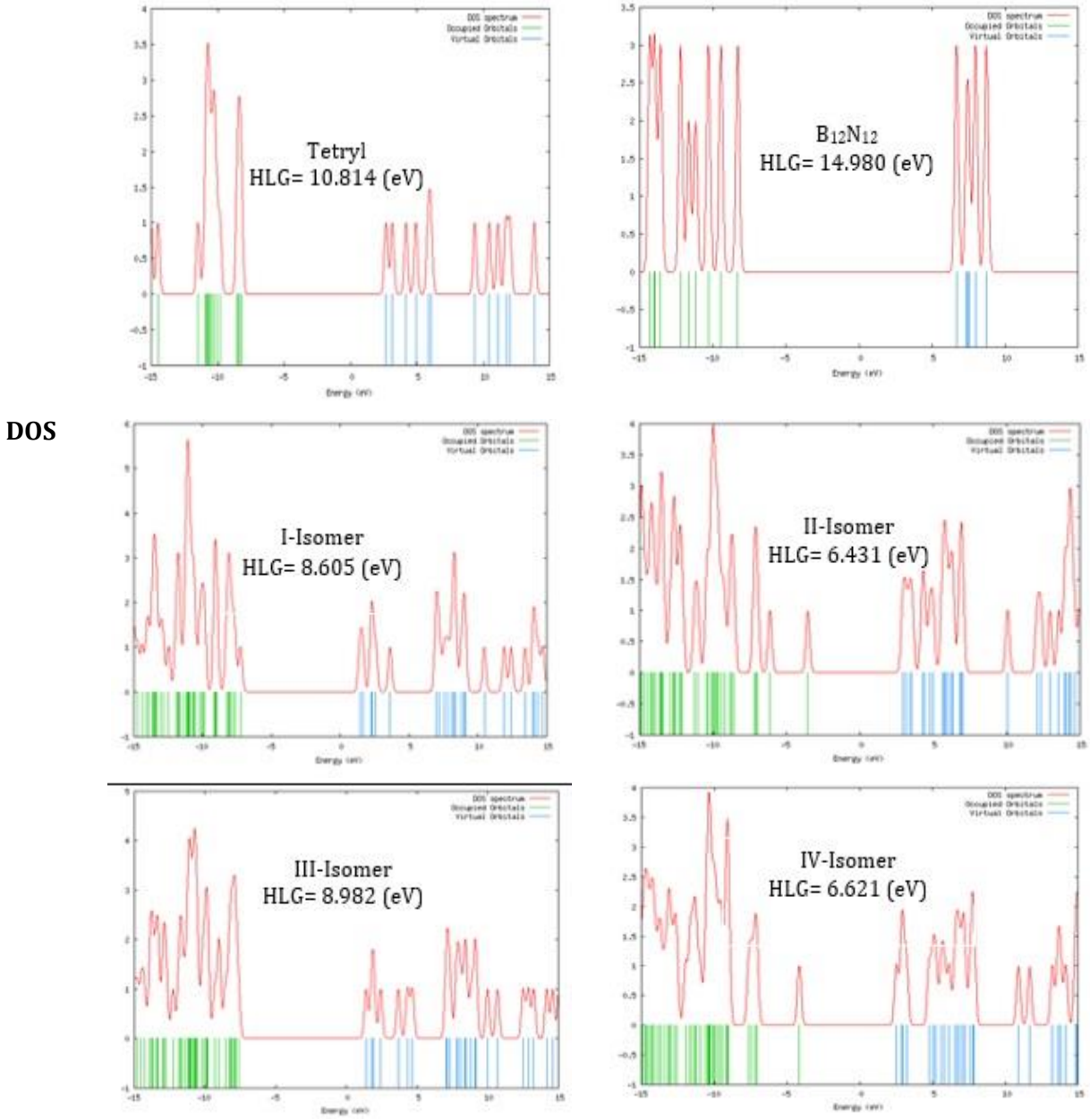

Figure 2. The density of states (DOS) diagrams for tetryl and its complexes with boron nitride cage

Conclusions

Tetryl is a toxic nitroaromatic explosive that has adverse effects on the health of human and other living organisms. Therefore, its detection and removal is of vital importance. In this regard, the adsorption of the tetryl on the surface of boron nitride cage was evaluated by DFT method in the

B3LYP/6-31G (d) level of theory. The results of the calculations revealed that the adsorption of tetryl on the surface of $B_{12}N_{12}$ is experimentally possible. In addition, the interaction of tetryl with boron nitride cage is exothermic as this nanostructure can be used for the thermal detection of tetryl. The effect of temperature on the studied process was also checked out and it was found out that 278.15 K is the optimum temperature. The obtained specific heat capacity values proved that tetryl adsorbing on the $B_{12}N_{12}$ leads to a significant decrease in the heat sensitivity. The structural properties including bond lengths and density values proved that the boron nitride cage complexes with tetryl have higher detonation velocity, blasting pressure and explosive power in comparison to pure tetryl. The frontier molecular orbital parameters also showed that boron nitride cage can be used as an electroactive sensing material for the determination of tetryl.

Acknowledgement

The author appreciates Islamic Azad University, Yadegar-e-Imam Khomeini (RAH) Shahre-Rey Branch, and Research Council for the support of this project.

Conflict of Interest

We have no conflicts of interest to disclose.

References

[1] Cady H.H. *Acta. Cryst.,* 1967, **23**: 601

[2] Hariharan P.C., Koski W.S., Kaufman J.J., Miller R.S. *Int. J. Quantum. Chem*., 1983, **23**:1493

[3] Harvey S.D., Fellows R.J., Campbell J.A., Cataldo D.A. *J. Chromatogr*., 1992, **605**:227

[4] Lindstorm I.E. *J. Appl. Phys*., 1970, **41**:337

[5] Mustafa A., Zahran A.A. *J. Chem. Eng. Data.,* 1963, **8**:135

[6] Myers S.R., Spinnato J.A. *Environ. Toxicol. Phar.,* 2007, **24**:206

[7] Ngoc Khue D., Lam T.D., Chat N.V., Bach V.Q., Minh D.B., Loi V.D., Anh N.V. *J. Ind. Eng. Chem.,* 2014, **20**:1468

[8] Ahmadi R., Pourkarim S., *Int. J. Bio-Inorg. Hybr. Nanomater.,* 2015, **4**:249

[9] Reddy T.V., Olson G.R., Wiechman B., Reddy G., Torsella J., Daniel F.B., Leach G.J. *Int. J. Toxicol*., 1999, **18**:97

[10] Fuller M.E., Kruczek J., Schuster R.L., Sheehan P.L., Arienti P.M. *J. Hazard. Mater.,* 2003, **100**:245

[11] Hilton J., Swanston C.N. *Br. Med. J.*1941, **2**:509

[12] Toal S. J., Trogler W. C., *J. Mater. Chem*., 2006, **28**:2871

[13] Stringer R.C., Gangopadhyay S., Grant S.A. *Anal. Chem*., 2010, **82**:4015

[14] Rodgers J.D., Bunce N.J. *Water Res.,* 2001, **35**:2101

[15] Heidary R. *J. Appl. Chem. Res*., 2013, **7**:21

[16] Pan Y., Zhu W., Xiao H. *Comput. Theor. Chem.,* 2017, **1114**:77

[17] Han G., Gou R.J., Ren F., Zhang S., Wu C., Zhu S. *Comput. Theor. Chem.,* 2017, **1109**:27

[18] Ma P., Pan Y., Jiang J.C., Zhu S.G. *Procedia. Eng.,* 2018, **211**:546

[19] Wang K., Fu X., Tang Q., Li H., Shu Y., Li J., Pang W. *Comp. Mater. Sci.,* 2018, **146**:230

[20] Sviatenko L.K., Gorb L., Shukla M.K., Seiter J.M., Leszczynska D., Leszczynski J., *Chemosphere.,* 2016, **148**:294

[21] Allis D.G., Zeitler J.A., Taday P.F., Korter T.M. *Chem. Phys. Lett.,* 2008, **463**:84

[22] Jain P., Sahariya J., Mund H.S., Sharma M., Ahuja B.L. *Comp. Mater. Sci.,* 2013, **72**:101

[23] Fayet G., Joubert L., Rotureau P., Adamo C. *Chem. Phys. Lett.,* 2009, **467**:407

[24] Konek C.T., Mason B.P., Hooper J.P., Stoltz C.A., Wilkinson J. *Chem. Phys. Lett.,* 2010, **489**:48

[25] Khaleghian M., Azarakhshi F. *Int. J. Nano. Dimens.,* 2016, **7**:290

[26] Bahrami A., Seidi S., Baheri T., Aghamohammadi M. *Superlattices. Micrstruct.,* 2013, **64**:265

[27] Baei M.T. *Comput. Theor. Chem.,* 2013, **1024**:28

[28] Esrafili M.D. *Phys. Lett.,* 2017, **381**:2085

[29] Vinu A., Mori T., Ariga K. *Sci. Technol. Adv. Mater.,* 2006, **7**:753

[30] Soltani A., Baei M.T., Mirarab M., Sheikhi M., Lemeshki E.T. *J. Phys. Chem. Solids***.,** 2104, **75**:1099

[31] Ahmadi R., Mirkamali E.S. *J. Phys. Theor. Chem. IAU Iran*., 2016, **13**:297

[32] Ahmadi R., Ebrahimikia M. *Phys. Chem. Res.,* 2017, **5**:617

[33] Shemshaki L., Ahmadi R. *Int. J. New. Chem.,* 2015, **2**:247

[34] Ahmadi R., Madahzadeh Darini N. *Int. J. Bio-Inorg. Hybr. Nanomater.,* 2016, **5**:273

[35] Ahmadi R., Shemshaki L. *Int. J. Bio-Inorg. Hybr. Nanomater.,* 2016, **5**:141

[36] Ahmadi R., Jalali Sarvestani M.R. *Phys. Chem. Res.,* 2018, **6**:639

[37] Jalali Sarvestani M.R., Ahmadi R. *Int. J. New. Chem.,* 2018, **5**:409

[38] Jalali Sarvestani M.R., Ahmadi R. *Int. J. New. Chem.,* 2017, **4**:400

[39] Ahmadi R., Jalali Sarvestani M.R. *Int. J. Bio-Inorg. Hybrid. Nanomater.,* 2017, **6**:239

[40] Ahmadi R. *Int. J. Nano. Dimens.,* 2107, **8**:250

[41] Culebras M., Lopez A.M., Gomez C.M., Cantarero A. *Sens. Actuators. A. Phys.,* 2016, **239**:161

[42] Mikkelsen S.R., Cortón E., Bioanalytical Chemistry. Wiley-Interscience: Michigan 2004; p 145

[43] Ahmadi R., Jalali Sarvetani M.R. *Iran. Chem. Commun.,* 2019, **7**:344

[44] Ravi P., Gore M.G., Tewari S.P., Sikder A.K. *Mol. Simulat.,* 2013, **38**:218

[45] Frisch M.J., Trucks G.W., Schlegel H.B., Scuseria G.E., Robb M.A., Cheeseman J.R., Scalman G., Barone V., Mennucci B., Petersson G.A., Nakatsuji H., Caricato M., Li X., Hratchian H.P., Izmaylov A.F., Bloino J., Zheng G., Sonnenberg J.L., Hada M., Ehara M., Toyota K., Fukuda R., Hasegawa J., Ishida M., T. Nakajima, Honda Y., Kitao O., Nakai H., Vreven T., Montgomery J.A., Jr., Peralta J.E., Ogliaro F., Bearpark M., Heyd J.J., Brothers E., Kudin K.N., Staroverov V.N., Kobayashi R., Normand J., Raghavachari K., Rendell A., Burant J.C., Iyengar S.S., Tomasi J., Cossi M., Rega N., Millam J.M., Klene M., Knox J.E., Cross J.B., Bakken V., Adamo C., Jaramillo J., Gomperts R., Stratmann R.E., Yazyev O., Austin A.J., Cammi R., Pomelli C., Ochterski J.W., Martin R.L., Morokuma K., Zakrzewski V.G., Voth G.A., Salvador P., Dannenberg J.J., Dapprich S., Daniels A.D., Farkas O., Foresman J.B., Ortiz J.V., Cioslowski J., Fox D. J.: Gaussian 09. Revision A.02 ed.; Gaussian, Inc.: Wallingford CT, 2009.

[46] Becke A.D. *J. Chem. Phys.,* 1993, **98**:5648

[47] Becke A.D. *Phys. Rev. A.,* 1998, **38**:3098

[48] Lee C., Yang W., Parr R.G. *Phys. Rev. B.,* 1998, **37**:785

[49] Farhang Rik B., Ranjineh khojasteha R., Ahmadi R., Karegar Razi M. *Iran. Chem. Commun.,* 2019, **7**:405

How to cite this manuscript: Mohammad Reza Jalali Sarvestani, Roya Ahmadi, Adsorption of Tetryl on the Surface of $B_{12}N_{12}$: A Comprehensive DFT Study. Chemical Methodologies 4(1), 2020, 40-54. DOI:10.33945/SAMI/CHEMM.2020.1.4.